Calculation of potential flow with separation in a right-angled elbow with unequal branches

By A. LICHTAROWICZ AND E. MARKLAND
Department of Mechanical Engineering, University of Nottingham

(Received 16 December 1961 and in revised form 16 May 1963)

A method developed by Roshko (1953*a*, *b*) has been applied to the case of flow round a right-angled elbow, in which the fluid separates at the inner corner at a speed which may be higher than the velocity of the separated flow far downstream. Numerical results have been evaluated and are presented for values of the ratio of the channel widths, downstream to upstream of the elbow, equal to 0·1 and 1·0.

The elbow may be regarded as one half of a two-dimensional representation of an axisymmetric plate valve, on which experiments indicate considerable variation in performance, the discharge coefficient being found to depend to a marked extent on the length of the valve land.

1. Introduction

The classical treatment of separated flows of an incompressible fluid as developed by Helmholtz and Kirchhoff often yields results which are in close agreement with experiments. The experimental result for the discharge coefficient of a sharp-edged orifice, for instance, agrees well with the calculated value of 0·61. For the case of an orifice, on the other hand, which is sufficiently long for the flow to reattach to the wall of the orifice, so that the separation zone becomes confined between the separating streamline at the front and a mixing region at the rear, the classical solution becomes inaccurate since the value of the pressure in the separated zone is no longer equal to that downstream. A similar condition exists in the case of separating flow past a normal flat plate, for which the Kirchhoff solution indicates a wake of indefinitely increasing width and a drag coefficient of 0·88, while experiments yield a drag coefficient of about 2·1 with a wake which, as is observed by Goldstein (1938) is not so wide as the calculated one.

Birkhoff (1950) discusses two variations of the Kirchhoff solution, in which the wake behind a flat plate is represented by a closed cavity, the pressure in which may be chosen to be lower than that in the free stream. More recently Roshko (1953*a*, *b*) has proposed an alternative solution in which the wake is of infinite length but of finite width, which is achieved by postulating that the speed of the fluid at separation from the corner of the plate is greater than the velocity in the undisturbed flow, and remains constant along a separation streamline which curves until the direction is restored to that of the undisturbed stream. From this point the separation streamline is straight and parallel to the direction of undisturbed flow. The pressure on the back of the plate is lower than the free-stream pressure; by suitably choosing the speed at separation the measured value of the base pressure may be introduced into the calculated solution, so obtaining a result which agrees well with experiments.

Roshko's concept of a free streamline along which the velocity along an initial curved portion is higher than the velocity far downstream has been applied by Whiteman (1956) to determine the discharge coefficient of a long orifice for a range of cavitation numbers, cavitation number being here defined as the ratio of back pressure to pressure drop across the orifice. Similar results have been derived by Bloomer *et al.* (1955) in connexion with entrances to channels, and Appel & Laursen (1953) have, in the same context, dealt with the case where there is an approach channel of finite width.

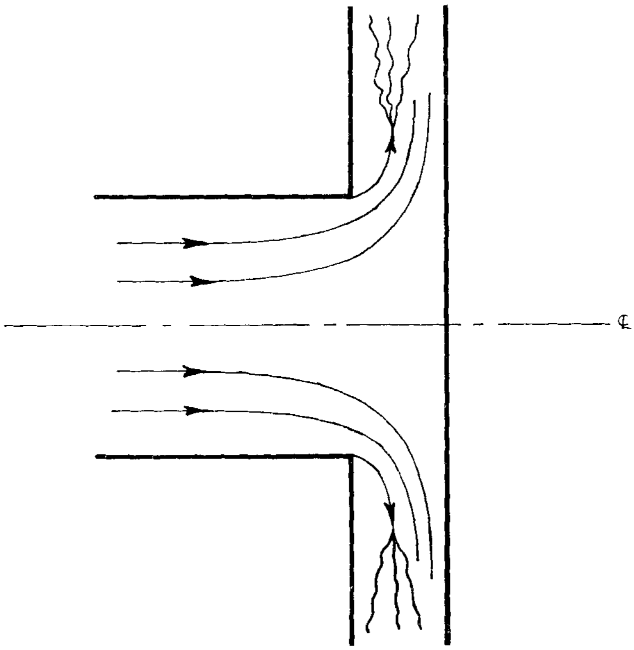

FIGURE 1. Schematic arrangement of plate valve.

The present work is concerned with the case of flow in a two-dimensional model of a plate valve, which consists of a pipe running full bore and discharging at its exit against a plate placed normal to the pipe axis, the required control of flow being achieved by varying the gap between the plate and the pipe exit. The valves are often made in such small sizes that the gap may be considerably less than the dimension of the flat land (see dimension l in figure 8) at the end of the pipe, so that, after separating from the right-angled corner, the fluid may reattach to the land as indicated on figure 1. In this event the pressure in the separation zone, which will be different from the downstream pressure, may be expected to be the primary factor determining the discharge coefficient. In the case of liquids the separation pressure cannot fall below the vapour pressure so that, under cavitating conditions, the discharge coefficient will be sensitive to the pressure level at which the valve is operating. The theoretical treatment given below was developed in conjunction with experiments involving cavitating and non-cavitating flow through a plate valve, in which large variations in discharge coefficient were noted, as described briefly in § 4. The work can also be applied to flow in a right-angled elbow with separation from the inner corner as considered by Haase (1954).

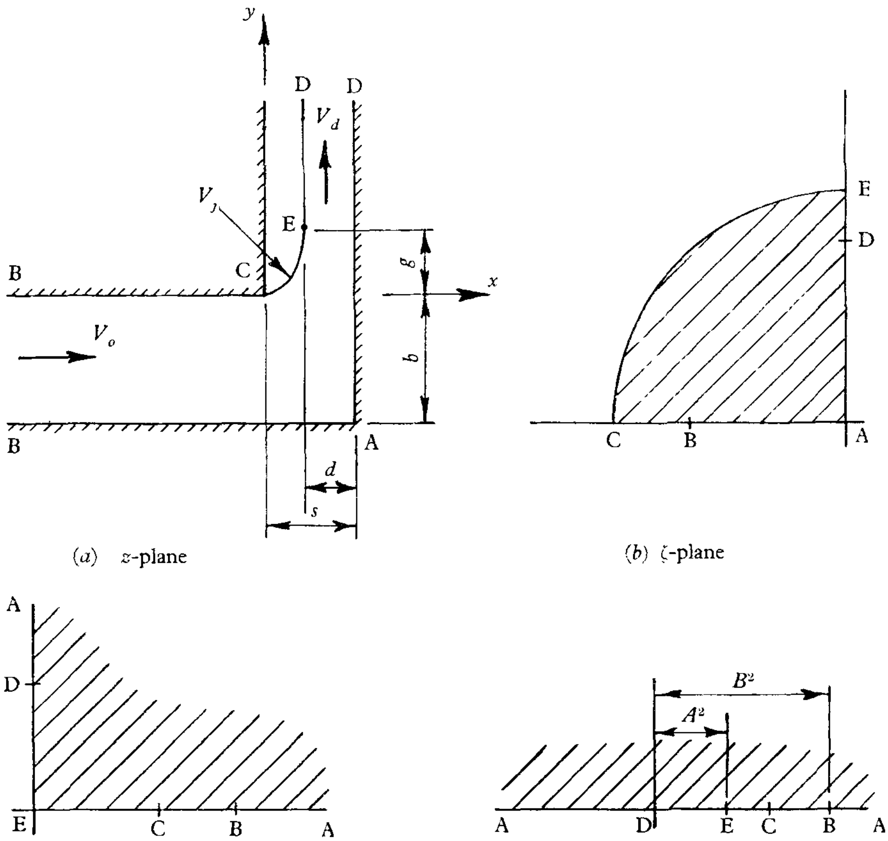

(*a*) z-plane (*b*) ζ-plane (*c*) χ-plane (*d*) t-plane

FIGURE 2. Notation and transformation planes.

2. Transformations and equations

Consider the flow in the z-plane round a right-angled elbow as shown on figure 2(*a*). The walls BC, BA and AD form the fixed boundaries; at C the flow separates and is bounded by the curved free streamline CE, which turns through a right-angle and along which the speed V_j is constant. The straight portion ED of the free streamline is parallel to AD and the velocity along it falls asymptotically from V_j at E to V_d. Writing, for convenience

$$V_j = kV_d = 1, \tag{1}$$

the velocity V_0 far upstream of the corner is given by

$$V_0 = d/bk, \tag{2}$$

where b and d are dimensions indicated on figure 2(*a*).

The appropriate conformal transformations are

$$dw/dz = -u+iv = -qe^{-i\theta} = \zeta, \tag{3}$$

$$\chi = -\tfrac{1}{2}(\zeta+1/\zeta), \tag{4}$$

and
$$t = (h^2+\chi^2)/(h^2+1) \tag{5}$$

in which
$$h = (k^2-1)/2k, \tag{6}$$

and these are illustrated on figure 2, the dimensions A^2 and B^2 in the t-plane being given by

$$A^2 = h^2/(h^2+1) \tag{7}$$

and
$$B^2 = (h^2+a^2)/(h^2+1), \tag{8}$$

where
$$a = \tfrac{1}{2}(V_0+1/V_0). \tag{9}$$

	z	ζ	χ	t
A	$s-ib$	0	∞ $i\infty$	$\pm\infty$
B	$-\infty\begin{smallmatrix}-ib\\+0\end{smallmatrix}$	$-V_0$	$a = \dfrac{1}{2}\left(V_0+\dfrac{1}{V_0}\right)$	$B^2 = \dfrac{h^2+a^2}{h^2+1}$
C	0	-1	1	1
D	$\begin{smallmatrix}s-d\\s\end{smallmatrix}+i\infty$	$\dfrac{i}{k}$	$ih = i\dfrac{k^2-1}{2k}$	0
E	$s-d+ig$	i	0	$A^2 = \dfrac{h^2}{h^2+1}$

TABLE 1

Table 1 lists the positions of corresponding points in the various planes. The flow in the t-plane corresponding to the required flow in the z-plane is from a source at B to an equal sink at D. The requisite source strength is $d/\pi k$, so the complex potential is

$$w = (d/\pi k)\{\log t - \log(t-B^2)\}. \tag{10}$$

Substitution in equations (3), (4) and (5) leads to

$$z = -\frac{d}{\pi k}\frac{1}{(1-A^2)^{\frac{1}{2}}}\int\{(t-1)^{\frac{1}{2}}+(t-A^2)^{\frac{1}{2}}\}\left(\frac{1}{t}-\frac{1}{t-B^2}\right)dt. \tag{11}$$

Choosing the constant of integration such that $z = 0$ when $t = 1$ yields the desired result

$$z = \frac{2d}{\pi k}\frac{1}{(1-A^2)^{\frac{1}{2}}}\left\{\begin{aligned}&\tan^{-1}(t-1)^{\frac{1}{2}}-(1-B^2)^{\frac{1}{2}}\tan^{-1}\left(\frac{t-1}{1-B^2}\right)^{\frac{1}{2}}\\&+A\tan^{-1}\frac{(t-A^2)^{\frac{1}{2}}}{A}-(A^2-B^2)^{\frac{1}{2}}\tan^{-1}\left(\frac{t-A^2}{A^2-B^2}\right)^{\frac{1}{2}}\\&-A\tan^{-1}\frac{(1-A^2)^{\frac{1}{2}}}{A}+(A^2-B^2)^{\frac{1}{2}}\tan^{-1}\left(\frac{1-A^2}{A^2-B^2}\right)^{\frac{1}{2}}\end{aligned}\right\}. \tag{12}$$

2.1. *The coefficient of contraction*

The ratio d/s may be regarded as a coefficient of contraction C_c, and may be evaluated by calculating from equation (12) the shape of the curved streamline CE, along which $1 \geqslant t \geqslant A^2$, and substituting for A and B in terms of k from (6), (7) and (8) as follows:

$$\frac{x}{s} = \frac{d}{\pi s}\left\{\begin{aligned} &\frac{k^2-1}{k^2}\tan^{-1}\frac{\{(k^2+1)^2t-(k^2-1)^2\}^{\frac{1}{2}}}{k^2-1} - \frac{k^2-1}{k^2}\tan^{-1}\frac{2k}{k^2-1} \\ &\qquad -\frac{2a}{k}\tanh^{-1}\frac{\{(k^2+1)^2t-(k^2-1)^2\}^{\frac{1}{2}}}{2ka} + \frac{2a}{k}\tanh^{-1}\frac{1}{a}\end{aligned}\right\}, \tag{13}$$

$$\frac{y}{s} = \frac{d}{\pi s}\left\{\frac{k^2+1}{k^2}\tanh^{-1}(1-t)^{\frac{1}{2}} - \frac{2}{k}(a^2-1)^{\frac{1}{2}}\tan^{-1}\frac{k^2+1}{2k}\left(\frac{1-t}{a^2-1}\right)^{\frac{1}{2}}\right\}. \tag{14}$$

At E, $$t = A^2 = \left(\frac{k^2-1}{k^2+1}\right)^2, \quad x = s-d = s(1-C_c),$$

and $y = g$ so that

$$\frac{1}{C_c} = 1 - \frac{k^2-1}{\pi k^2}\tan^{-1}\frac{2k}{k^2-1} + \frac{2a}{\pi k}\tanh^{-1}\frac{1}{a}, \tag{15}$$

$$\frac{g}{s} = C_c\frac{k^2+1}{\pi k^2}\tanh^{-1}\frac{2k}{k^2+1} - \frac{2C_c}{\pi k}(a^2-1)^{\frac{1}{2}}\tan^{-1}(a^2-1)^{-\frac{1}{2}}. \tag{16}$$

Equations (15) and (16) give the position in the z-plane of E, the point at which the curved free streamline is tangential to the subsequent straight portion. For potential flow the discharge coefficient C_D is equal to the contraction coefficient C_c; for a real fluid C_D will differ from C_c by an amount which depends on the Reynolds number of the motion.

2.2. *Velocity and pressure distribution along the free streamline*

The speed along the curved part CE of the streamline is constant, and has been taken as unity in the analysis. Beyond E, the velocity falls asymptotically from unity to $1/k$. The variation of velocity along ED may be found as follows

$$\frac{dw}{dz} = \frac{dw}{dt}\frac{dt}{dz} = \frac{k^2+1}{2k}\{(t-1)^{\frac{1}{2}} - (t-A^2)^{\frac{1}{2}}\}, \tag{17}$$

in which $A^2 \geqslant t \geqslant 0$ along ED. The component velocities along ED are thus

$$u = 0 \quad \text{and} \quad v = \frac{k^2+1}{2k}\left[(1-t)^{\frac{1}{2}} - \frac{\{(k^2-1)^2-(k^2+1)^2t\}^{\frac{1}{2}}}{k^2+1}\right]. \tag{18}$$

The corresponding values of x and y along ED are found, after some reduction, from equation (12) to be

$$x/s = 1 - C_c,$$

$$\frac{y}{s} = \frac{C_c}{\pi}\left\{\begin{aligned} &\frac{k^2+1}{k^2}\tanh^{-1}(1-t)^{\frac{1}{2}} - \frac{2}{k}(a^2-1)^{\frac{1}{2}}\tan^{-1}\frac{k^2+1}{2k}\left(\frac{1-t}{a^2-1}\right)^{\frac{1}{2}} \\ &+\frac{k^2-1}{k^2}\tanh^{-1}\frac{\{(k^2-1)^2-(k^2+1)^2t\}^{\frac{1}{2}}}{k^2-1} - \frac{2a}{k}\tan^{-1}\frac{\{(k^2-1)^2-(k^2+1)^2t\}^{\frac{1}{2}}}{2ka}\end{aligned}\right\}. \tag{19}$$

For any chosen value of t within the specified range the position along the free streamline and the velocity at this position may be calculated. A similar procedure may be adopted to determine the velocity along any of the walls.

It is convenient to express static pressure p at any point in the form of a dimensionless pressure coefficient $C_p = (p - p_d)/\frac{1}{2}\rho V_d^2$. From (1) and Bernoulli's equation it follows that

$$C_p = 1 - k^2 V^2, \tag{20}$$

where V is the local velocity.

3. Computed results

Figures 3–6 show graphically the results of computations for a range of parameters s/b and k.*

The contraction coefficient given in table 2 is seen from figure 3 to be insensitive in changes in s/b up to about 0·3, the flow for small valve openings approximating to the limiting case of discharge from a large reservoir with stagnation pressure

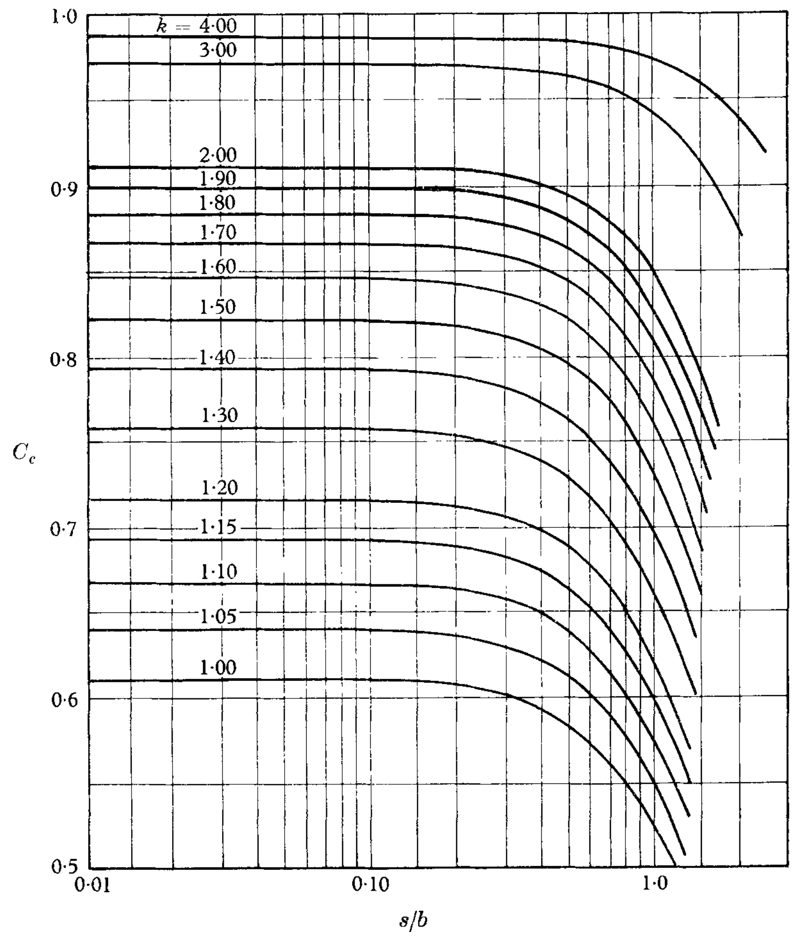

FIGURE 3. Variation of C_c with s/b for various values of k.

* Results with other values of s/b and k have been computed and are available.

k \ s/b	0·01	0·1	0·5	0·8	1·0	1·2
1·0	0·6110	0·6098	0·5842	0·5507	0·5255	0·5000
1·1	0·6679	0·6666	0·6391	0·6029	0·5757	0·5480
1·2	0·7166	0·7154	0·6871	0·6496	0·6212	0·5921
1·4	0·7928	0·7916	0·7645	0·7276	0·6990	0·6692
1·6	0·8466	0·8455	0·8216	0·7879	0·7610	0·7324
1·8	0·8846	0·8837	0·8634	0·8339	0·8098	0·7835
2·0	0·9116	0·9109	0·8940	0·8689	0·8479	0·8245
3·0	0·9708	0·9705	0·9638	0·9534	0·9440	0·9329
4·0	0·9872	0·9871	0·9841	0·9792	0·9748	0·9695

TABLE 2. Values of contraction coefficient C_c

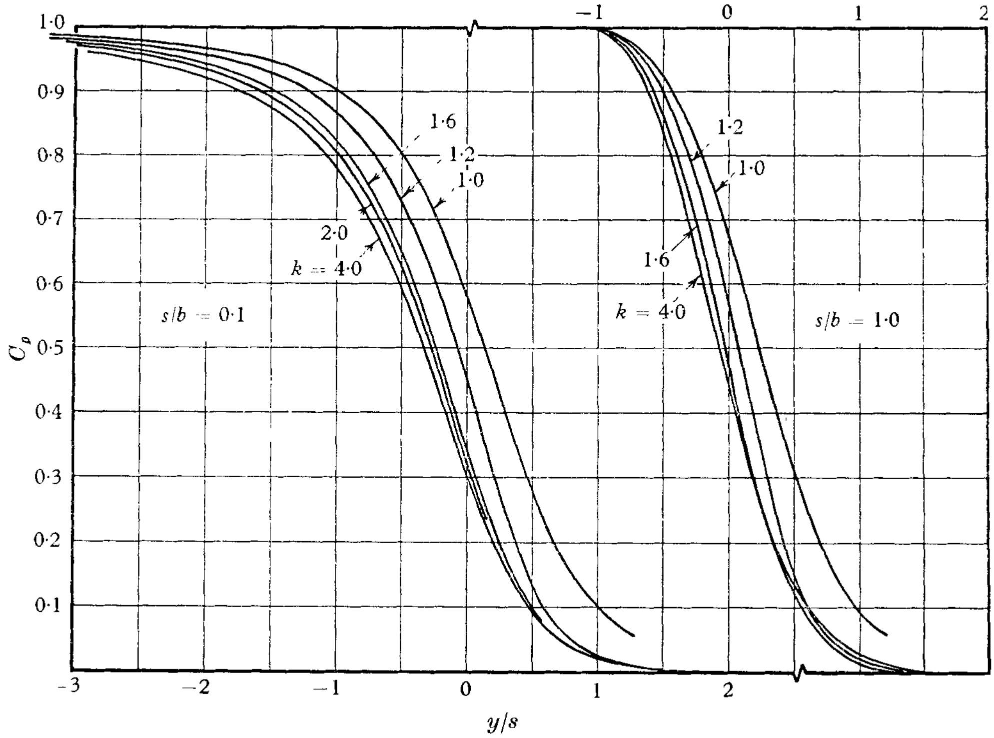

FIGURE 4. Pressure distribution along wall AD for various values of k.

extending over most of the plate facing the pipe, as may be seen from figure 4. The insensitivity of C_c to s/b over the practical operating range of plate valves has important implications. Consider a valve working at constant inlet and outlet pressures p_b and p_d. The pressure p_j along CE in figure 2 is given by

$$\frac{p_d - p_j}{p_b - p_d} = \frac{k^2 - 1}{1 - C_c^2(s/b)^2}; \tag{21}$$

thus if cavitation determines p_j (so that the left-hand side of this equation is constant) k will decrease as s/b is increased, though the decrease of k will be fairly small for values of s/b up to about 0·5. For instance, if $k = 2$ when $s/b = 0{\cdot}1$, reference to figure 3 shows that increasing s/b to 0·5 decreases k to about 1·86.

If cavitation does not occur and $p_d - p_j$ is governed by a turbulent reattachment process, k will be roughly constant and independent of $p_b - p_d$, provided that the orifice land is long enough to achieve full pressure recovery at reattachment.

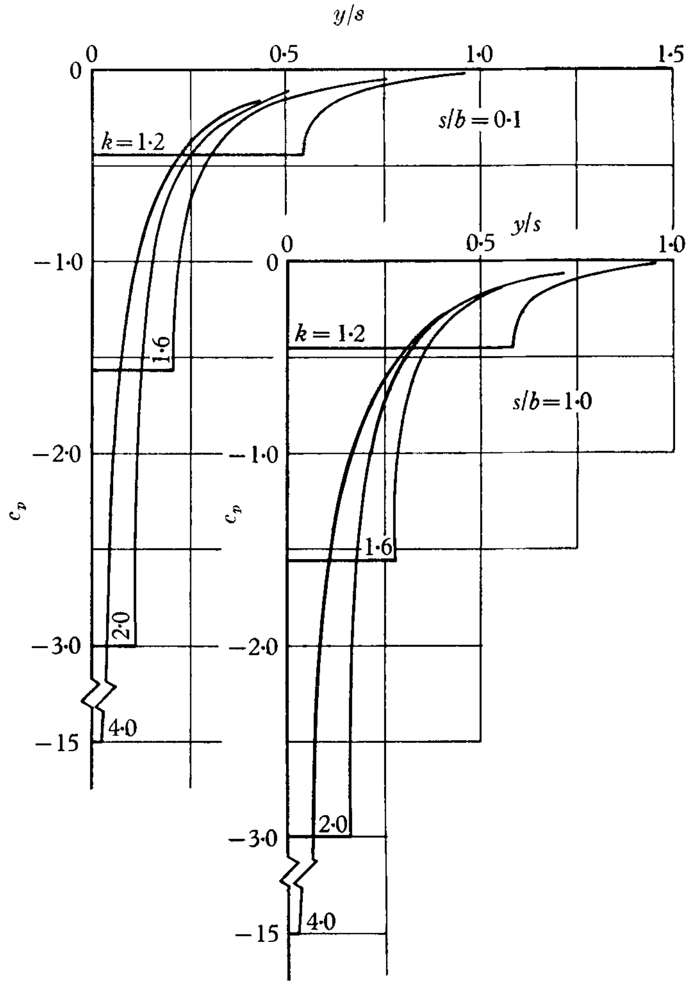

FIGURE 5. Pressure distribution along the separating streamline for various values of k.

If it is not long enough to do so, k will decrease as s increases. Thus for all the usual flow conditions k will either remain roughly constant or will decrease as s is increased. The falling off in figure 3 at about $s/b = 0{\cdot}3$ of the curves of C_c for constant k can thus be interpreted as an increasing loss of control as the plate moves away from the land.

The effect of changes in k on contraction coefficient and free-streamline shape is most pronounced when k is close to unity (where 1 % change in k produces about 1 % change in C_c). When reattachment occurs under non-cavitating conditions, the shape of the separating streamline taken from figure 6, with an appropriate value of k, may be expected to give a fair approximation in the neighbourhood of the corner to the separating flow of a real fluid, although the discontinuity in

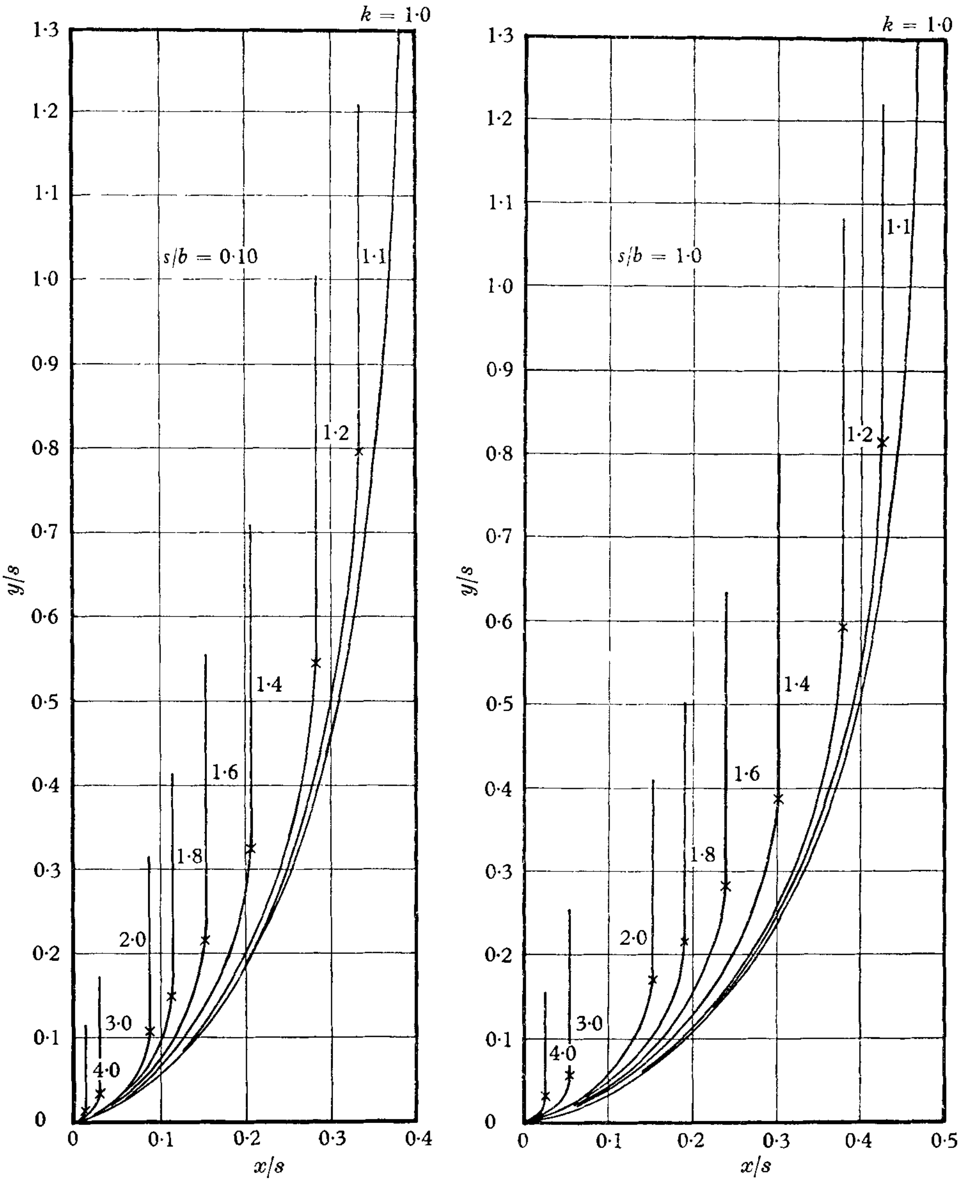

FIGURE 6. Separation streamline for various values of k.

pressure gradient at E along the separating streamline illustrates discontinuity in velocity gradient which would not be expected in a real flow.

As the value of k increases the length of the constant-pressure zone contracts, tending to the limiting case of unseparated flow with infinitely negative pressure at the corner C as $k \to \infty$.

4. Experiments on a plate valve

The foregoing analysis arose from experiments on an axisymmetric plate valve. Although pressures along the land could not be measured with sufficient accuracy to make worthwhile comparisons with the results of calculations, some typical discharge coefficients are shown in figures 7 and 8, for their incidental interest. The lower curve of figure 7 indicates a non-cavitating flow system in which reattachment does not take place on the land; under non-cavitating conditions the appropriate value of k is unity and the value of C_c obtained from

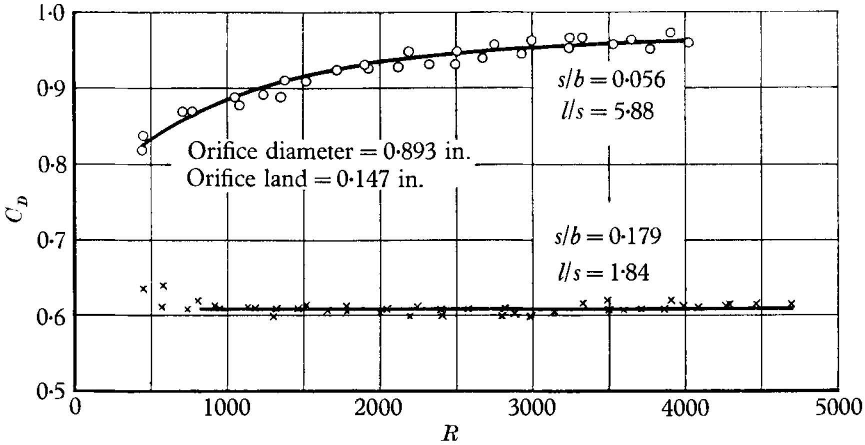

FIGURE 7. Variation of C_D with Reynolds number for an axisymmetric plate valve; the Reynolds number is defined in terms of the discharge Q and the orifice diameter D by $R = Q/\pi D\nu$.

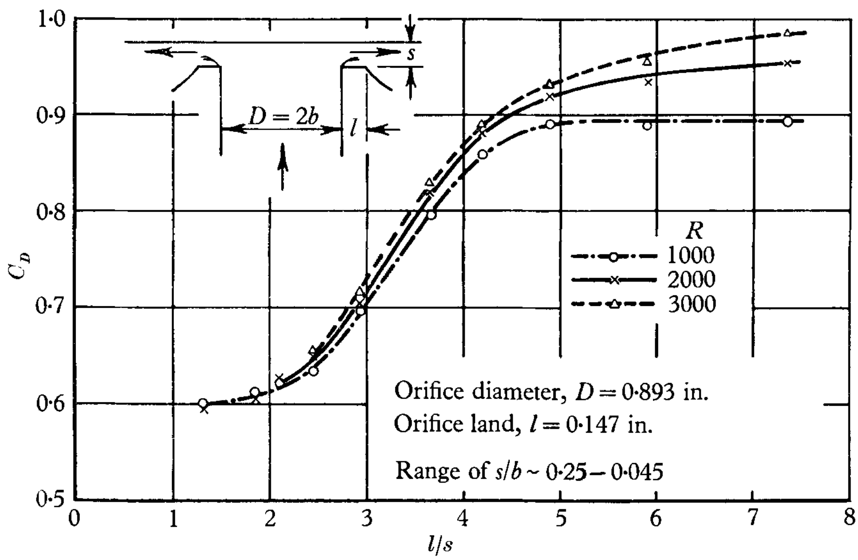

FIGURE 8. Variation of C_D with land/gap ratio in an axisymmetric plate valve.

figure 3 for the corresponding two-dimensional flow agrees well with the measured value of C_D. The upper curve indicates flow with reattachment, in which the pressure recovery, demonstrated by changes in C_D, varies with the Reynolds number R to a significant extent. Figure 8 shows that pressure recovery in the reattaching flow depends strongly on the land length. Although a smooth transition is shown from separated to reattached flow as l/s increases, some cases of instability were noted in which, at fixed valve geometry and fixed R, two flow patterns were possible, depending on whether the condition were approached by increasing or decreasing the flow; such a characteristic is undesirable if the valve is to be used as a control device. The effect of cavitation was to decrease C_D, the decrease being more pronounced in the regime of reattached flow.

The authors wish to express their gratitude to Rolls-Royce Ltd, for providing assistance during the work on the project, which was conducted at the University of Nottingham.

REFERENCES

APPEL, D. W. & LAURSEN, E. M. 1953 Free-streamline analysis of transition flow and jet deflection. *State Univ. of Iowa, Studies in Engng, Bull.* no. 35, p. 21.

BIRKHOFF, A. 1950 *Hydrodynamics.* New York: Dover.

BLOOMER, N. T. *et al.* 1955 Design of two-dimensional entrances to hydraulic channels. *The Engineer*, **199**, 265.

GOLDSTEIN, S. 1938 *Modern Developments in Fluid Dynamics.* Oxford University Press.

HAASE, D. 1954 Strömung in einem 90°-Knie. *Ingen. Arch.* **22**, 282.

ROSHKO, A. 1953*a* A new hodograph for free-streamline theory. *N.A.C.A. Tech. Note* no. 3168.

ROSHKO, A. 1953*b* On the drag and shedding frequency of two-dimensional bluff bodies. *N.A.C.A. Tech. Note* no. 3169.

WHITEMAN, K. J. 1956 Free-streamline theory and its application to flow through orifices. *Brit. Hydromech. Res. Assoc.* TN no. 539.